Brightness Dependent Properties of Gamma Ray Bursts

Boris Stern [1,2], Juri Poutanen[2,3], and Roland Svensson[2]

ABSTRACT

Brightness dependent correlations have been conclusively detected in the average time profiles of gamma-ray bursts (GRBs). Determining the time constants of the stretched exponential slopes of the average peak-aligned time profile of GRBs as a function of the peak brightness, we find that the post-peak slope shows time dilation when comparing bright and dim bursts, while the pre-peak slope hardly changes. Stronger bursts are thus more symmetric than weaker bursts at a high confidence level. The very weakest bursts have a different shape (i.e., a different stretched exponential index) of their average time profile as compared to brighter bursts. This difference is too large to be explained by trigger effects and Poisson noise. We interpret these correlations as being the result of an intrinsic positive correlation between brightness and complexity of GRBs. This interpretation is directly confirmed by simulations as well as by a morphological classification of bursts. The fact that such a correlation can be observed should impose new constraints on the distribution of GRBs over luminosity distance.

Subject headings: Gamma ray bursts – Methods: data analysis

1. Introduction

Although gamma-ray bursts (GRBs) are quite diverse in their properties (e.g., Fishman & Meegan 1995), clues to their origin may be hidden in the average statistical properties of GRBs. Mitrofanov et al. (1993, 1995) introduced a useful average function of light curves of GRBs. This is the average peak-aligned profile, i.e., the sum of individual time profiles aligned at their highest peaks and normalized to their peak count rates. This function was used in searches for the time dilation effect (also see Norris et al.1994). Stern (1996) found that the average post-peak time profile has a simple "stretched" exponential shape, $F(t) \propto \exp[-(t/t_{\rm d})^{1/3}]$, where t is the time measured from the peak of the event, and $t_{\rm d}$ is a decay time constant. This fact, besides providing a possible clue for understanding the time variability of GRBs (Stern & Svensson 1996), gives an excellent opportunity to study such effects as time dilation and time asymmetry of GRBs. These

[1]Institute for Nuclear Research, Russian Academy of Sciences Moscow 117312, Russia, stern@al20.inr.troitsk.ru

[2]Stockholm Observatory, S-133 36 Saltsjöbaden, Sweden, stern@astro.su.se, juri@astro.su.se, svensson@astro.su.se

[3]Uppsala Observatory, Box 515, S-75120 Uppsala, Sweden

effects were previously studied using different methods (e.g., Nemiroff et al. 1994; Norris 1996 and references therein).

Stern (1996) used the stretched exponentiality of the average time profile to study the time dilation of its post-peak slope. Here we extend that study with a more accurate procedure for the data analysis, using a larger sample of GRBs, and considering both the pre-peak and the post-peak slopes. Another recent advantage is the access to the pulse avalanche model developed by Stern & Svensson (1996), which successfully describes many statistical properties of GRBs including the stretched exponential shape of the average time profile, and, of particular importance for the present work, the root-mean-square (rms) variance of individual time profiles. This means that we can rely on this model when estimating the errors of stretched exponential fits, which in turn gives us reliable estimates of the significance levels of any observed effects.

2. Data Analysis

This work is based on the publically available data in the Compton Gamma-Ray Observatory data archive in Goddard Space Flight Center. Our sample includes bursts up to trigger number 3745 and contains 912 useful events. All time profiles are constructed using 64 ms time resolution data from the Large Area Detectors (LAD) together with 1.024 s resolution extensions to earlier and later times.

We use the count rates summed over the four LAD energy channels, covering the 25 – 1000 keV energy range, as well as the count rates in channels 2+3 (50 – 300 keV). The advantage of the wider energy band is that it should reduce possible effects of the spectral redshift if the photon spectrum has a "convex" shape (which is usually the case). On the other hand, channels 2 and 3 have a better signal to noise ratio. We study the general behavior of the average time profile using the wider energy band, and investigate the average shape of weak bursts using only channels 2 and 3.

The procedure of background fitting included a visual examination of all bursts together with an analysis of all ambiguous signal variations to establish whether they came from the same direction as the main burst. We discarded those bursts, for which a reliable reconstruction of the signal for 50 s before and 125 s after the main peak was not possible due to interfering background variations or data gaps. When possible we used two widely separated background fitting windows ($[-120\,\mathrm{s}\ ,\ -70\,\mathrm{s}]$ and $[+200\,\mathrm{s}\ ,\ +250\,\mathrm{s}]$ relative to the trigger). In order to estimate the accuracy of the fitting procedure we measured residuals to the background fits for channels 2 and 3 in windows located approximately in the middle of the fitted time interval avoiding possible contributions of a GRB signal. We made this test for the 176 weakest events. The residuals normalized to the peak GRB fluxes are distributed in a symmetric Gaussian-like curve with an average value of $+1.4 \times 10^{-3}$ and a rms deviation of 0.0187. The latter can be interpreted as the typical relative error of the fit for an individual profile. The statistical error of the sum of relative residuals is $\pm 1.5 \times 10^{-3}$ - this is a rough estimate of the total uncertainty of the background for the average

time profile of weak GRBs. The most difficult source of a possible bias for the weakest events are background variations on the same time scale as GRBs which could be mixed with the GRB signal. Our impression is that after we cleaned out events with bad background such a bias is small. We cannot, however, quantify this conclusion. A test repeating the procedure using rescaled events added to real samples of the background is necessary for such a quantitative estimate. For bright events the fitting dependent errors are negligible.

When sorting bursts into brightness groups, we used the peak fluxes for 64 ms time resolution in the BATSE-3 catalog (Meegan et al. 1996). Peak alignment and peak normalization of bursts were performed using count rates in 64 ms time resolution. We developed a flexible scheme where each count rate excess over neighboring time intervals is tested for its statistical significance. The shortest time scale in which the peak domination over its neighborhood is significant was used to localize the peak. The test for the brightness independency of the results obtained with such a procedure is described below.

The parameters of an average time profile are derived from stretched exponential fits, $F(t) = \beta \exp[-(t/t_0)^\nu]$, where, β and t_0 are fitting parameters, and the index ν was free if its best fit value is of interest and was set to 1/3 when determining the t_0. The value 1/3 does not necessarily have a special meaning, the 1σ confidence interval is $\nu = 0.34 \pm 0.02$. If we set $\nu = 0.32$ or $\nu = 0.36$ then t_0 changes (by factor 1.5 for $\nu = 0.36$), however its ratio for different brightness groups remains the same within 4% accuracy.

Because the sample of all detected GRBs is too small to estimate the errors of the average time profiles, we used the *pulse avalanche* model of Stern & Svensson (1996) both to find a reasonable likelihood function for the fitting procedure and to estimate the statistical errors. We found that the statistical errors are robust against variations of the model parameters. For the sample sizes used in our analysis, the statistical errors can be expressed as $\sigma(t_{\rm r,d})/t_{\rm r,d} = 0.201\sqrt{100/N}$, $\sigma(t_{\rm d} + t_{\rm r})/(t_{\rm d} + t_{\rm r}) = 0.196\sqrt{100/N}$, and $\sigma(t_{\rm d}/t_{\rm r})/(t_{\rm d}/t_{\rm r}) = 0.135\sqrt{100/N}$, where $t_{\rm r}$ and $t_{\rm d}$ are the time constants for the pre-peak (rising) and post-peak (decaying) slopes of the average time profile, respectively, and N is number of events in a sample. The better accuracy of $t_{\rm d}/t_{\rm r}$ is caused by the strong correlation between the two slopes. The errors exceed the error estimates in earlier works (e.g., in Stern 1996, they were underestimated by a factor 1.5). Large statistical errors when extracting time constants are natural if GRBs are produced by a near-critical process as is described by the pulse avalanche model of Stern & Svensson (1996) In the case of exact criticality, the time constants completely disappear. Note that our estimates of the statistical errors are, formally, model-dependent. However, the model simultaneously describes reasonably well the average time profile, the autocorrelation function, and the rms variance of individual profiles (Stern & Svensson 1996). Then it can be argued that our error estimates are also correct.

3. The Average Time Profile for Different Brightness Groups

The average peak-aligned time profiles for three brightness groups are shown in Figure 1. Our stretched exponential fits are given in Table 1 and in Figure 2. The rising (pre-peak) slope is steeper for all brightness groups, but the asymmetry is increasing when going from the bright to the dimmest group.

In order to check a possible brightness dependent bias for t_0, we rescaled strong bursts to the brightness ranges of the weaker samples, simulating noise and trigger operations. A parent sample consisting of the 268 brightest events has $t_{\rm d} = 0.503$. After rescaling to the weaker samples 3, 4, 5, and 6, it has $t_{\rm d} = 0.500$, 0.498, 0.510, and 0.525, respectively. Thus the possible bias is less than the statistical errors by an order of magnitude . The trigger efficiencies for samples 3, 4, 5 and 6 are 0.993, 0.93, 0.77, and 0.38, respectively.

Let us for the time being ignore the weakest sample 6. The strongest effect is the time dilation of $t_{\rm d}$ by a factor $1.85^{+0.82}_{-0.57}$ (90% confidence interval) if one compares samples 1 and 7. The rejection level for a null hypothesis (i.e., no time dilation) is 0.998. The rising slope, on the other hand, hardly changes and the variations of $t_{\rm r}$ do not exceed the statistical errors. This leads to a rising asymmetry for weaker samples as quantified by the asymmetry ratio, $t_{\rm d}/t_{\rm r}$. Comparing samples 1 and 7 gives $(t_{\rm d}/t_{\rm r})_{\rm dim}/(t_{\rm d}/t_{\rm r})_{\rm bright} = 1.48^{+0.55}_{-0.32}$ (90% confidence interval). A careful estimate of the significance level using model simulations gives 0.985. The time dilation of $t_{\rm r} + t_{\rm d}$ being $(t_{\rm r} + t_{\rm d})_{\rm dim}/(t_{\rm r} + t_{\rm d})_{\rm bright} = 1.56^{+0.63}_{-0.36}$ (obtained by comparing samples 1 and 7) has a statistical significance of 0.99. The value is in a good agreement with recent results of Norris (1996), however the definition of time dilation is too uncertain when strong shape-brightness correlations are observed.

Note that all effects are significant only relative to the brightest end of the GRB brightness distribution. If one removes the 64 brightest bursts, the effects almost disappear - only marginally significant indications remain. This is, however, natural as the brightest bursts cover a wide range of peak brightnesses on a logarithmic scale (see Fig. 2). The asymmetry-brightness correlation cannot be explained as a trigger effect, as the trigger efficiency is high throughout the brightness range where we see this correlation. It could not result from spectral redshift as our measurements of the time asymmetry in separate LAD energy channels do not show any dependency on the energy channel (Stern et al. 1997).

The weakest sample 6 apparently has a different shape of its average time profile which is characterized by a stretched exponential index, $\nu = 0.45$, while the other samples have $\nu \sim 0.33$ (in each energy channel). We tested whether the difference can results from trigger selection biases and from effects of Poisson noise. As a reference weak sample, we used a sample (denoted as 8) including the 197 weakest events with the peak count rates in the range 0 – 120 $\rm bin^{-1}$. The best fit value of the stretched exponential index for sample 8 is $\nu = 0.47$ (channels 2 and 3). The average trigger efficiency for strong events rescaled to the peak count rate interval of sample 8 is 0.57. The index of the "rescaled" average time profile is $\nu = 0.37$. The deformations of the time profile after this procedure are of the same sign as that distinguishing samples 6 and 8 from

brighter samples, but are much less than required to account for the difference in ν.

To find the rejection level for the hypothesis that the peculiar $\nu = 0.47$ for sample 8 is the combined result of the trigger-associated bias and a statistical fluctuation, we performed model simulations taking into account Poisson noise and trigger selection effects. The resulting rejection level is close to 0.99 (3 out of 600 simulated samples gave $\nu > 0.47$). However we cannot rely on this estimate because we have other possible uncertainties.

First, we could have both statistical and systematic errors in the background fit which can affect ν. If we add to the average profile a constant 0.0015, which is our estimate of the fitting statistical error (see the residuals test in §2), then the rejection level drops to 0.97 (or, ifwe admit an error of 0.003, then $\nu = 0.447$ and the rejection level becomes 0.94). Second, some profile-dependent biases could be accumulated in the various steps of the "data processing chain". Such steps include: 1) the classification of a trigger as a burst; 2) the inclusion of its 64 ms record into the database; and 3) the adding of the burst to the useful sample. According to Meegan (1996) the selection at steps 1) and 2) is not affected by any features of the burst temporal structure. We admit that we may have introduced a selection bias at step 3) at the level of 2 – 4 events. With these uncertainties we carefully characterize the significance of the peculiar ν for sample 8 as a "2σ indication" (~ 0.95).

4. Interpretation of Correlations

GRBs consist of a number of pulses of different durations but similar shapes. Let all these pulses have locally independent sources of energy. Then if two pulses coincide in time, their amplitudes sum up. In a complex event hundreds of pulses are piling up, increasing the peak brightness by perhaps an order of magnitude. Then simple events are on average intrinsically weaker than complex events. At the same time, simple events are asymmetric just because a single pulse in general is asymmetric with a sharp rise and a slower decay (e.g., Norris et al. 1996). This asymmetry is washed out in complex events where the position of the highest peak is more or less random among many overlapping pulses (a possible "global" asymmetry where brighter pulses tend to appear earlier remains). Furthermore, the sum of peak-aligned single pulse events gives $\nu \sim 0.5$.

To demonstrate that this kind of correlation appears in the pulse avalanche model, we simulated a large sample of "bursts" using a set of model parameters fitted to the average time profile for the full sample of all real bursts. The results are given in Table 2, where one can see the tendencies of a larger asymmetry ratio, $t_{\rm d}/t_{\rm r}$, and a larger stretched exponential index, ν, for weaker events, as well as the effect of "time shrinking", which is opposite to the observed time dilation. The latter implies a new positive correction for the observed time dilation.

5. Complexity vs Observed Brightness

If correlations between the average time profile and brightness can be explained by complex bursts being intrinsically brighter than simple bursts, then it is of interest to classify bursts according to their complexity and then check whether any correlations exist between complexity and observed brightness. Lestrade (1994) using the number of runs "up" and "down" in GRB time profiles as a measure of complexity did not find such correlations. Actually this is a difficult problem: all events should be rescaled to the same low brightness to avoid brightness-dependent biases, but then the effect is difficult to extract due to the large Poisson noise. We found that the only way to detect correlations is to concentrate on the simplest events dominated by a single smooth pulse having a sharper rise and a slower decay. Such pulses can be be recognized due to their "canonical" shape even at a high Poisson noise.

To make a brightness independent classification we rescaled all 912 events to the same peak count rate range (125 – 150 bin^{-1} in all energy channels), adding proper Poisson noise. As it is important to conduct such a classification as a "blind test", we arranged the procedure in such a way that none of the test persons knew the actual peak amplitude of a displayed burst. All persons stated their decisions independently.

As a fine classification at high Poisson noise is impossible, we restricted the classification to two main classes: (1) "simple" single pulse events (see definition above), and (2) "complex" events. Doubtful and too short events were not included into these classes.

The test was performed by three persons: A, B and C. All test persons demonstrated the same tendency: events classified as "simple" are systematically dimmer than those classified as "complex". A Kolmogorov-Smirnov test for the two brightness distributions of "simple" and "complex" bursts gave the following consistency levels (i.e., the probability that the two distributions are drawn from the same parent distribution): A – $0.75 \cdot 10^{-2}$, B – 0.28, C – $0.43 \cdot 10^{-2}$, A $\times$ C (i.e., only those events where A and C agreed) – $0.38 \cdot 10^{-2}$. The test directly confirms that complex events dominate the bright range and simple bursts dominate the weakest range (see Fig. 3).

Some systematic bias of this test is still possible for the weakest bursts having peak count rates below 125 bin^{-1} as they have worse signal to noise ratios than rescaled events. The total number of such events is, however, small (74 out of 912 events).

We also performed a similar computer test using a χ^2 threshold as the criterium for the event to be dominated by a single pulse. The parametrization of Norris et al. (1996) was used as the fitting hypothesis for single "canonical" pulses with the additional imposed requirement that the best fit exponential decay time constant for an individual pulse is larger than the corresponding rise time constant. The result of this test is surprisingly close to that of the visual test: "complex" events are systematically brighter at the 0.997 confidence level. Details will be given in Stern, Poutanen & Svensson (1997).

6. Conclusions and Discussion

The effects we confidently detect can be summarized as follows: 1.) The strongest bursts have peculiarly short time constants (confidence level $> 99\%$). 2.) The strongest bursts have peculiarly small asymmetry between the rising and the decaying slopes of the average time profile (confidence level 98 – 99%). 3.) The weakest bursts ($F_{\rm p} \lesssim 0.8\,{\rm ph\,cm^{-2}\,s^{-1}}$) have a peculiar shape of the decay slope of their average time profile, which can be characterized by a large stretched exponential index (a formal estimate gives a 99% confidence level, a more realistic estimate is 2σ). 4.) Events consisting of a single pulse are systematically weaker than complex events (99.5% confidence level).

Effect 1) can be interpreted as the widely discussed time dilation effect. Unfortunately other observed effects complicate its treatment. Therefore we can only state that after applying all possible corrections the value of the time dilation lies between 1.5 and 4 and that an unknown fraction of this is due to an intrinsic anti-correlation between brightness and duration (see Brainerd 1994).

Effects 2) and 3) have a common qualitative interpretation as being produced by an intrinsic correlation between the number of pulses in a burst and its peak brightness. This interpretation is directly supported by 4) and by model simulations.

All these effects by themselves are not as important as the constraints one can put on the distribution of GRBs over luminosity distance due to the fact that we do observe these effects. If some of GRB's properties correlate with their intrinsic luminosity, this condition alone does not mean that we are able to observe such a correlation. The second necessary condition is that the distribution of GRBs over luminosity distance is not a power law. This is necessary in order for the ratio of intrinsically weak and intrinsically strong events to change at some apparent brightness range. As for the brightest range of GRBs this is more or less evident – in the cosmological scenario a transition to Euclidean scaling with a power law index $-3/2$ should exist and this is indicated by the data (e.g., Meegan et al. 1996).

The domination of intrinsically weak bursts in the weakest range would imply a less trivial turnover of the distance distribution towards larger distances. Indeed, a relative deficit of intrinsically strong bursts at the weakest end of the brightness distribution indicates that we are sensing the edge of the spatial distribution of GRBs. In a cosmological scenario this could imply strong evolution. Effect 3) which leads to such a conclusion is measured near the threshold of the detector sensitivity where one has to deal with many possible biases. This makes effect 3) less significant than the other effects listed above.

Nevertheless we believe that effect 3) is real as it is supported by effect 4). It certainly should be studied more attentively, maybe using untriggered bursts in 1024 ms records. As is often the case, the most difficult fraction of the data can be the most valuable. We suggest that weak GRBs deserve more attention.

We thank Cecilia Albertsson and Felix Ryde for helpful assistance and Ed Fenimore and Charles Meegan for useful discussions. We are grateful to the referee, Robert Nemiroff, for valuable remarks. This research used data obtained from the HEASARC Online Service provided by the NASA/GSFC. This study was supported by grants from the Swedish Royal Academy of Sciences, the Swedish Natural Science Research Council, and a NORDITA Nordic Project grant.

#	Peak flux	N	$t_{\rm d}$	$t_{\rm r}$	$t_{\rm d}+t_{\rm r}$	$t_{\rm d}/t_{\rm r}$
1	12.5 – 200	64	0.42±0.10	0.36±0.09	0.78 ±0.18	1.17 ±0.19
2	3 – 12.5	193	0.60±0.08	0.40±0.06	1.00 ±0.13	1.50 ±0.11
3	1.75 – 3	159	0.75±0.11	0.37±0.06	1.12 ±0.16	2.02 ±0.21
4	1 – 1.75	241	0.72±0.09	0.46±0.06	1.18 ±0.14	1.56 ±0.13
5	0.7 – 1	139	0.85±0.14	0.48±0.08	1.33 ±0.21	1.89 ±0.18
6	0 – 0.7	116	0.80±0.14	0.37±0.07	1.17 ±0.20	2.16 ±0.26
7	0.75 – 2.5	463	0.78±0.07	0.45±0.06	1.22 ±0.11	1.73 ±0.10

Table 1: Time constants of the average time profiles

Note. — Time constants, $t_{\rm r}$ and $t_{\rm d}$ [s], of the stretched exponential fit to the pre-peak (rising) and post-peak (decaying) average time profiles, respectively. Peak fluxes [$\rm ph\,cm^{-2}\,s^{-1}$] taken from the BATSE data base for the sum of channels 2 and 3. N is the number of bursts in a given brightness interval. Errors obtained using the estimates in §2 correspond to 1σ.

Peak flux	$t_{\rm d}$	$t_{\rm r}$	$t_{\rm d}+t_{\rm r}$	$t_{\rm d}/t_{\rm r}$	ν
$0-\infty$	0.66	0.41	1.07	1.61	0.34
$3-\infty$	0.75	0.68	1.43	1.10	0.26
0.8 – 3	0.72	0.50	1.22	1.44	0.31
0 – 0.8	0.50	0.19	0.69	2.63	0.48

Table 2: Fitting parameters of the average time profiles for simulated bursts

Note. — The fitting parameters, $t_{\rm r}$, $t_{\rm d}$, and ν, of the average time profiles for simulated bursts in different "intrinsic brightness" intervals. The amplitude of a single pulse is sampled uniformly in the $[0,1]$ interval. The stretched exponential index, ν, is given for the $0.75 < t^{1/3} < 4$ fitting interval. The parameter values are model-dependent, and are given only as an example.

REFERENCES

Brainerd, J.J. 1994, ApJ, 428, L1

Fishman, G. J., & Meegan, C. A. 1995, ARA&A, 33, 415

Lestrade, J. P. 1994, ApJ, 429, L5

Meegan, C. A. 1996, private communication

Meegan, C. A., et al. 1996, ApJS, 106, 65

Mitrofanov, I. G. et al. 1993, in AIP Conf. Proc. 280, Compton Gamma-Ray Observatory, eds. M. Friedlander, N. Gehrels, & D. J. Macomb (New York: AIP), 761

Mitrofanov, I. G., Pozanenko, A. S., Chernenko, A. M., Fishman, G. J., Kouveliotou, C., Meegan, C. A., Paciesas, W. S., & Sagdeev, R. Z. 1995, Astronomy Reports, 39, 305

Nemiroff, R. J., Norris, J. P., Kouveliotou, C., Fishman, G. J., Meegan, C. A., & Paciesas, W. S. 1994, ApJ, 423, 432

Norris, J. P., Nemiroff, R. J., Scargle, J. D., Kouveliotou, C., Fishman, G. J., Meegan, C. A., Paciesas, W. S., & Bonnell, J. T. 1994, ApJ, 424, 540

Norris, J. P. 1996 in Proc. Third Huntsville Gamma-Ray Burst Workshop (New York: AIP)

Norris, J. P., Nemiroff, R. J., Bonnell, J. T., Scargle, J. D., Kouveliotou, C., Paciesas, W. S., Meegan, C. A., & Fishman, G. J. 1996, ApJ, 459, 393

Stern, B. E. 1996, ApJ, 464, L111

Stern, B. E., & Svensson, R. 1996, ApJ, 469, L109

Stern, B. E., Poutanen, J., & Svensson, R. 1997, in preparation

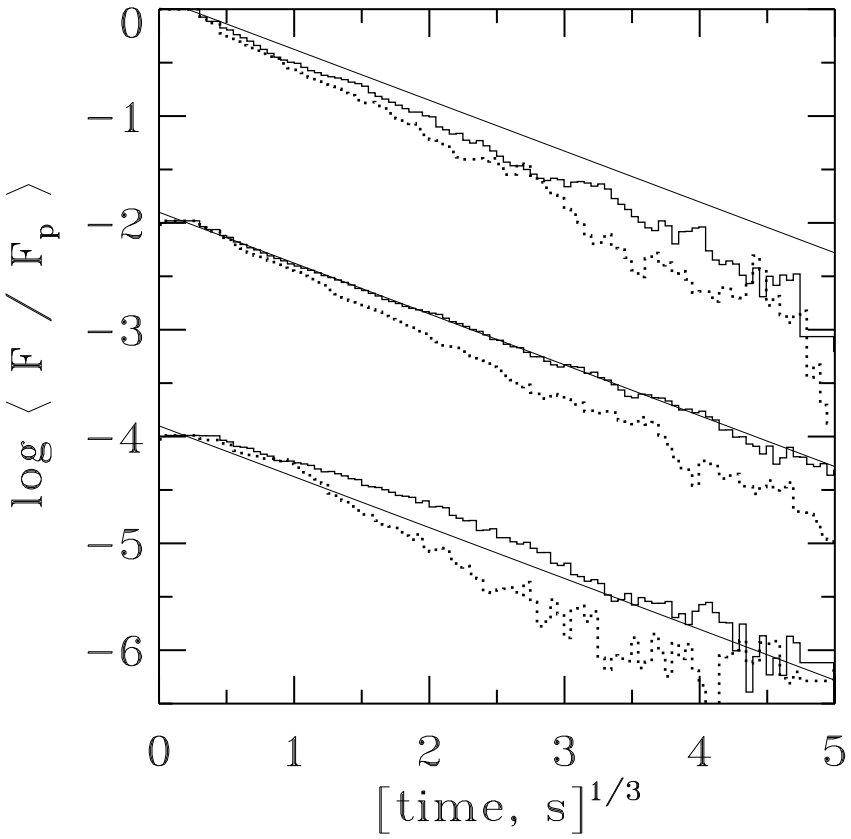

Fig. 1.— Average peak-aligned time profiles for three brightness groups: 1) Peak photon flux $F_{\rm p} > 5\,{\rm ph\,cm^{-2}\,s^{-1}}$, 157 GRBs (upper curves); 2) $0.7 < F_{\rm p} < 5$, 630 GRBs (middle curves); and 3) $F_{\rm p} < 0.7$, 116 GRBs (lower curves). Average time profiles for medium and low brightness groups are shifted downwards for clarity. Solid and dotted curves represent the average post-peak and pre-peak time profiles, respectively. Straight lines show the best linear fit to the post-peak history of the medium brightness group. The best fit time constants are $t_{\rm r} = 0.35$ s, $t_{\rm d} = 0.50$ s for the brightest group; $t_{\rm r} = 0.43$ s, $t_{\rm d} = 0.74$ s for the medium group; and $t_{\rm r} = 0.37$ s, $t_{\rm d} = 0.80$ s for the weakest group. See caption for Fig. 2 regarding the weakest sample.

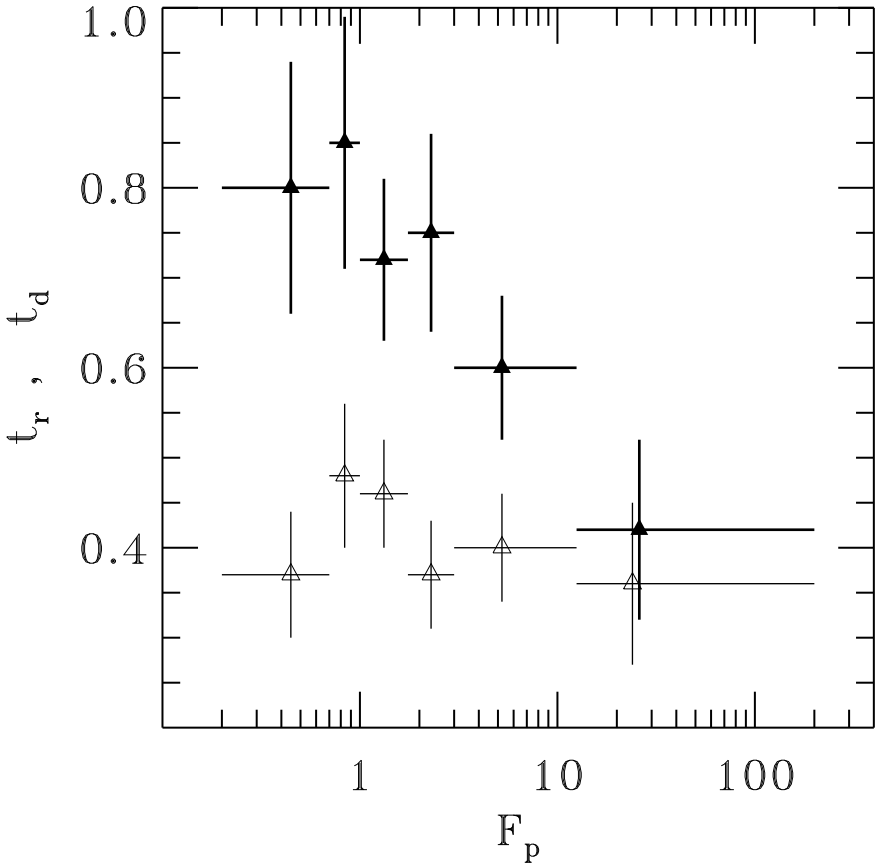

Fig. 2.— Time constants, t_r and t_d, vs. peak photon flux, F_p, in 64 ms time resolution. Lower and upper crosses represent t_r and t_d for the pre-peak (rising) and post-peak (decaying) average time profiles, respectively. Error bars of the time constants correspond to 1σ. Error bars in photon flux represent the width of the brightness groups. The values for the weakest sample (# 6 in Table 1) are not trustworthy because the average time profile apparently has a different shape as compared to the stretched exponential function (see Fig. 1).

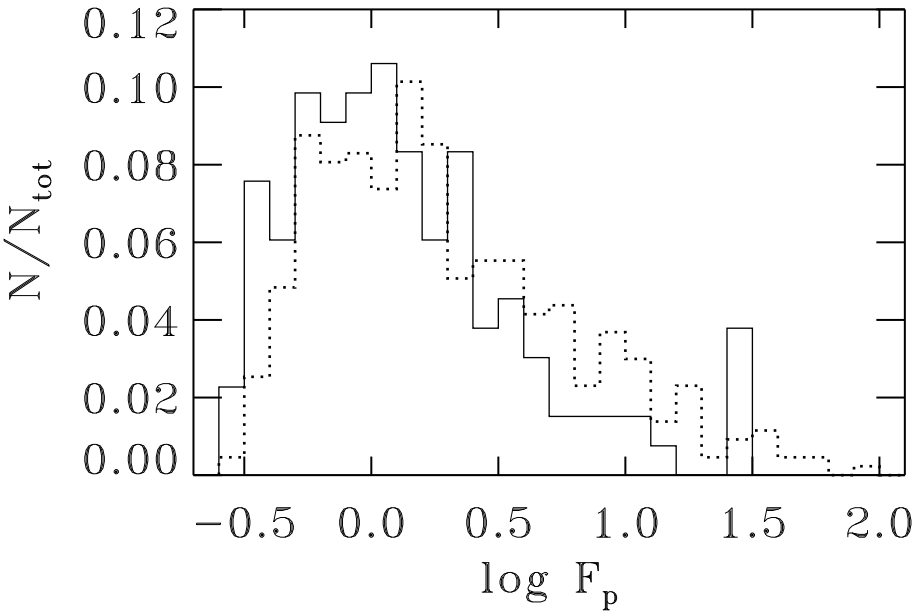

Fig. 3.— The normalized peak brightness distributions of bursts classified by both of the test persons A and C as "one pulse events" (solid histogram) and as "complex events" (dotted histogram). $N_{\rm tot}$ is the total number of bursts in respective class.